Inverse Unified Power Quality Conditioner: Investigations towards its Performance and Capabilities

M. Hosseini Abardeh and R. Ghazi

Abstract: The cost of switching devices increases exponentially by increasing their rating. Hence, attractiveness of using unified power quality conditioners (UPQC) is reduced when compensation to be carried out for high power sensitive loads. In this paper, a new configuration for UPQC is presented. Using the fundamental power flow analysis, it is shown that by interchanging the position of series and parallel part of UPQC, the total rating of compensator decreases. To acquire more rating reduction, a new simple control algorithm is presented for voltage compensation by injecting the reactive power. Using numerical simulations, the performance of proposed and conventional configurations is compared to show their operational effectiveness and limitations in different loads and network conditions.

Keywords: Unified power quality conditioner, UPQC, inverse unified power quality conditioner, I-UPQC, active power filter, power quality.

1. Introduction

A great part of total generated electric power is used by industrial consumers. These kinds of costumers need a reliable and high quality power for proper operation. On the other hand, their nonlinear nature causes current distortion that deteriorates distribution systems components and generates voltage distortion as passes through the network impedance. The voltage distortion like harmonic, sag and swell can interrupt many industrial activities by affecting the sensitive devices.

Active power filters (APFs) have been used in three last decades to compensate the voltage and current quality problems. Parallel active power filters (PAPFs) can eliminate current distortions caused by loads and perform power factor correction. On the other hand, to protect sensitive consumers from voltage distortions, series active power filters (SAPFs) are used [1].

There exist four trends to enable the more efficient utilization of APFs for protecting the high power loads and networks against power quality disturbances. They are described as follows:

Improvement of manufacturing technology of APF's semiconductor switches to reduce the cost and increase the rating.

Application of hybrid configurations of active and passive power filters. The passive part compensates low order disturbances and the active part eliminates high order harmonics. In this way, the rating of APF is greatly reduced because it does not deal with all harmonics [2].

Using the selective harmonic compensation algorithms to minimize the rating of series and parallel APFs. Depending on the network structure and its characteristics, some harmonics give rise to more severe problems. Focusing only on compensation of critical harmonics (like the ones which excite system resonance frequency)the total rating of APF will be reduced [3,4].

Optimization of APF power flow by using the energy optimized control algorithms. The angle between the injected voltage by SAPF and the current passes though it can be optimized to minimize the active power exchange between APF and network which can reduce its rating [5,6].

By connecting a SAPF and a PAPF through their dclink, a unified power quality conditioner (UPQC) is produced [7] as shown in Fig. 1(a). Each part consists of a voltage source inverter (VSI) which generates compensating voltages and currents. This device can simultaneously compensates voltage distortions like sag, swell, flicker, current harmonics and reactive power in distribution system [8,9].

There exist two distinct control strategies to generate the reference waveforms for series part of UPQC. If the injected voltage is in phase with the source current, the voltage compensation is achieved by the active power. If the injected voltage is orthogonal to the source current, the reactive power is used to achieve the voltage compensation [10].

The main contribution of current paper is introducing a new power quality conditioner device named inverse unified power quality conditioner (I-UPQC). The conventional UPQC in which the series part is at the network side is compared with an inverse unified power quality conditioner where the series part is at the load side as shown in Fig. 1(b). The active and reactive power control strategies are compared and their effects on the device rating are analyzed.

In the next section, the flow of active power in UPQC and I-UPQC is analyzed during occurrence of a voltage sag and swell. Then in section III, by considering the same voltage sag condition, the total rating of UPQC and I-UPQC is compared. In section IV, the control algorithms for generating the reference waveforms of series and

Manuscript received November 6, 2012, revised January 23, 2013.

M. Hosseini Abardeh and R. Ghazi are with the Department of Electrical Engineering, Ferdowsi University of Mashhad, Mashhad, Iran.

The correspondent author's email is: rghazi@um.ac.ir

parallel part of UPQC and I-UPQC are presented. Finally, in section V the performance of two configurations is examined using numerical simulations. The necessary comparison is also made in this section.

2. Power Flow Analysis

The amount of active power drawn from the network by shunt component of UPQC and I-UPQC during sag depends on the power that is fed into the network by their series components. This power is dependent on the angle of the voltage injected by the series part and the current passes through the series transformer. If the voltage generated by series VSI has the same angle as that of the source current, the compensator injects real power into the network to regulate the load voltage. As the angle between the source current and the injected voltage increases, the active power injected by the series part decreases, so the shunt part draws less active power from network. In this condition the voltage regulation is performed by injecting reactive power which is generated by the series VSI.

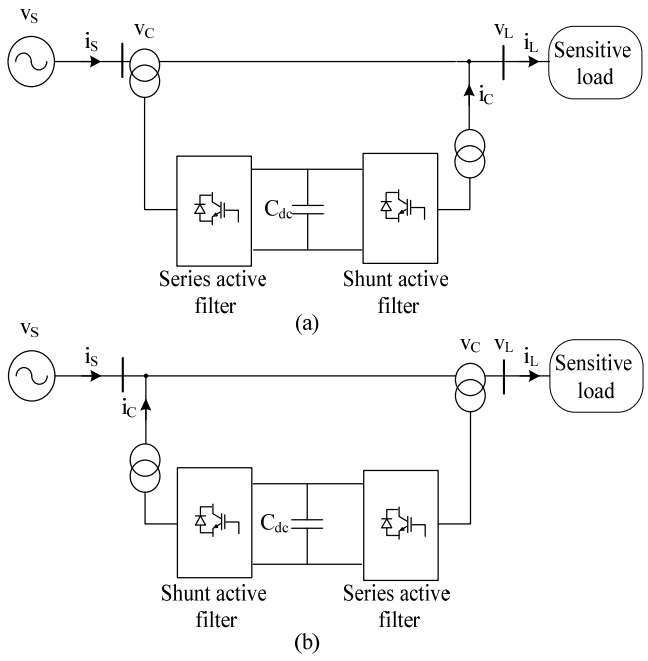

Fig. 1. Configuration of (a) UPQC and (b) I-UPQC

Identical to UPQC, during sag, I-UPQC draws active power (*PShunt*) from the network by its shunt part and injects it (*PSereis*) into the network by its series part as shown in Fig. 2. The reverse process occurs during voltage swell. As can be seen from Fig. 3, when voltage swell occurs, the shunt component injects active power which is drawn by series component.

3. Rating Analysis

Rating of UPQC and I-UPQC can be calculated by fundamental frequency power flow analysis. Suppose our aim is to compensate *x* p.u. sag or swell. As the voltage sag is more common in distribution networks, here their rating are calculated only for operation in sag condition. The same procedure can be used to calculate the compensators rating when the voltage swell occur.

A. Rating of UPQC

Due to common DC link between shunt and series parts of the UPQC, active power can flow between two parts. When a sag occurs, the shunt component draws active power (*PShunt*) from the network and the series component injects it (*PSereis*) to the network as shown in Fig. 4. The reverse process occurs during the voltage swell.

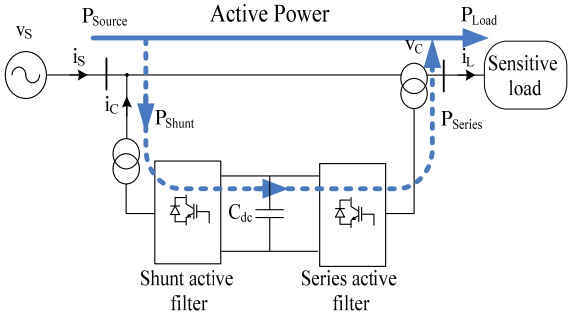

Fig. 2. Power flow in I-UPQC during voltage sag.

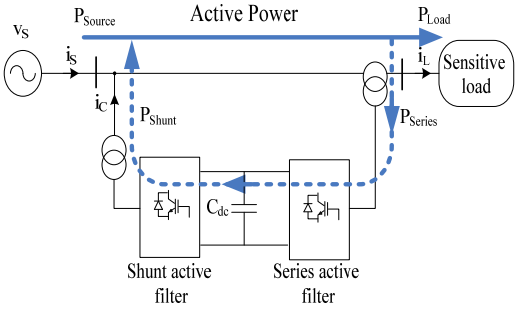

Fig. 3. Power flow in I-UPQC during voltage swell.

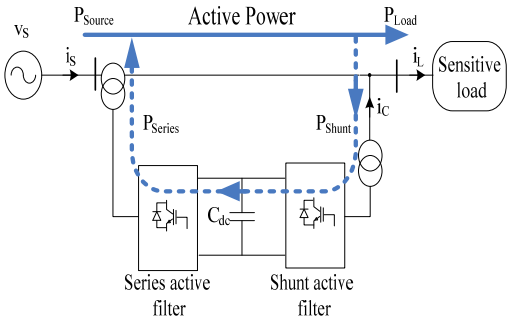

Fig. 4. Power flow in UPQC during voltage sag.

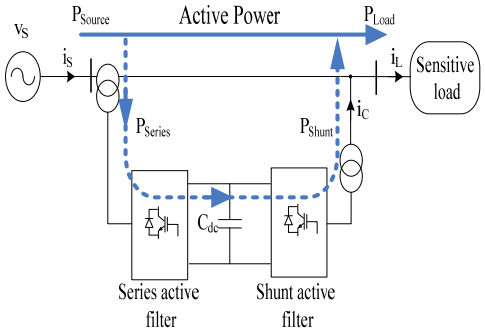

Fig. 5. Power flow in UPQC during voltage swell.

As can be seen from Fig. 5, when the voltage swell occurs, the shunt component injects active power which is drawn by the series component. The power demand of the total system is equal to the sum of load power and the internal losses of UPQC, i.e.,

$$P_{Source} + P_{Shunt} = P_{Load} + P_{Series} + P_{Loss} \tag{1}$$

where *PLoss* consists of switching and copper losses of the coupling transformers.

Suppose that the amplitude of the source voltage and load current is equal to 1.0 p.u. and *x* is the sag amplitude, then we have

$$\begin{aligned} V_{S1} &= V_{L1} = 1.0 \text{ p.u.} \\ I_{L1} &= I_{L2} = 1.0 \text{ p.u.} \\ V_{S2} &= (1-x)V_{S1} \text{ p.u.} \end{aligned} \tag{2}$$

where subscripts *L* and *S* correspond to load and source, 1.0 and 2.0 represent the quantities before and during sag. Respectively if the SAPF of the UPQC generates all reactive power needed by load, the angle between source voltage and current will be zero, i.e.,

$$V_S I_S \cos(0) = V_L I_L \cos\phi \tag{3}$$

where ϕ is the angle between fundamental component of load current and voltage. Therefore as shown in Fig. 6 the UPQC injects *IC1* into the network to compensate the load reactive power. When the voltage sag occurs the series part maintains the load voltage constant therefore, the load power remains constant before and during voltage sag, i.e.,

$$V_L I_L \cos\phi = V_{S1} I_{S1} = V_{S2} I_{S2} \tag{4}$$

Therefore, the current drawn from source during sag would equals to

$$I_{S2} = \frac{V_L I_L \cos\phi}{(1-x)V_{S1}} \tag{5}$$

The current of SAPF can be calculated by (6) using trigonometry of the vector diagram of Fig. 6, i.e.,

$$\begin{aligned} I_{C2} &= (I_{L1}^2 + I_{S2}^2 - 2I_{L1}I_{S2}\cos\phi)^{0.5} \\ &= \left(\frac{(1-x)^2 + (2x-1)\cos^2\phi}{(1-x)} \right)^{0.5} \end{aligned} \tag{6}$$

The shunt filter voltage can be calculated by (7),

$$V_{Shunt} = V_S + Z_{shunt} I_{C2} \tag{7}$$

In this equation *Zshunt* is the equivalent impedance of shunt coupling transformer which is supposed to be 0.1 p.u. Therefore the rating of the shunt component is

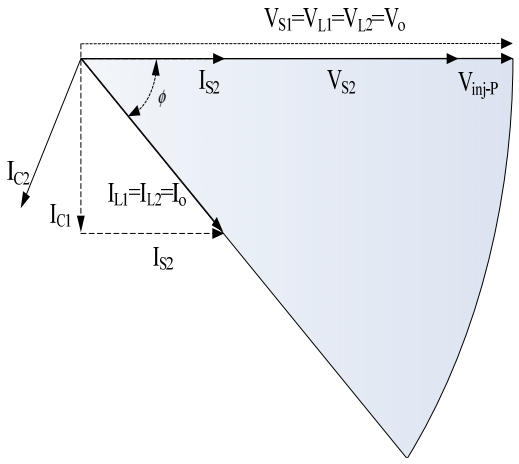

Fig. 6. Phaser diagram of voltage compensation by injecting active power.

$$S_{shunt} = (V_S + Z_{shunt} I_{C2}) I_{C2} \tag{8}$$

Substitution of (6) into (8) yields

$$\begin{aligned} S_{shunt} &= V_{shunt} I_{shunt} \\ &= \frac{\left((1-x)^2 + (2x-1)\cos^2\phi\right)}{(1-x)} \\ &+ Z_{shunt} \frac{(1-x)^2 + (2x-1)\cos^2\phi}{(1-x)^2} \end{aligned} \tag{9}$$

When the UPQC injects active power into the network, the angle between injected voltage and the network voltage is zero, i.e.,

$$V_{inj-P} = V_C = xV_S \tag{10}$$

Using (5) and (10) and considering *VS*=1.0 p.u, we have

$$S_{series} = V_C I_{S2} = \frac{x\cos\phi}{1-x} \tag{11}$$

and the total rating of UPQC is the sum of *Sshunt* and *Sseries*, i.e.,

$$S_{UPQC} = S_{shunt} + S_{series} \tag{12}$$

This is the rating of the UPQC when it is designed to compensate the voltage sags as large as *x* p.u. by injecting active power into the network. If the reactive power is injected into the network to regulate the voltage, the amplitude of the injected voltage is calculated by following equation using the trigonometry of vectors shown in Fig. 7

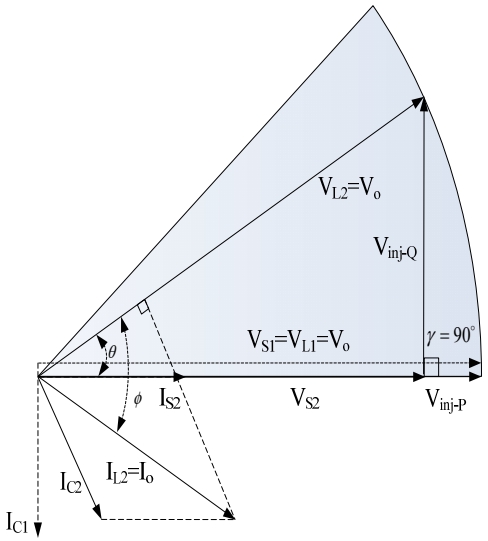

Fig. 7. Phaser diagram of voltage compensation by injecting reactive power.

$$V_{inj-Q} = V_C = \sqrt{V_{S1}^2 - V_{S2}^2} = \sqrt{2(2-x)} \tag{13}$$

In Fig. 7, *IC1* shows the injected current to compensate for the load reactive current when the network voltage is normal.

The current passes through the series transformer is equal to (5). Hence, the rating of the SAPF is given by following;

$$S_{series} = V_{inj-Q} . I_{series} = \frac{\sqrt{x(2-x)}}{1-x}\cos\phi \tag{14}$$

The current of the shunt filter *IC2* equals;

$$\begin{aligned} I_{C2} &= \sqrt{I_{L2}^2 - I_{S2}^2 - 2I_{L2}I_{S2}\cos(\phi-\theta)} \\ &= \frac{\sqrt{(1-x)^2 + \cos^2\phi - 2(1-x)\cos\phi\cos(\phi-\theta)}}{1-x} \end{aligned} \tag{15}$$

Then, the voltage of the SAPF can be calculated using (8). The rating of SAPF can be obtained by productof its voltage and current as follows;

$$\begin{aligned} S_{shunt} &= \frac{\sqrt{(1-x)^2 + \cos^2\phi - 2(1-x)\cos\phi\cos(\phi-\theta)}}{1-x} \\ &+ \frac{(1-x)^2 + \cos^2\phi - 2(1-x)\cos\phi\cos(\phi-\theta)}{(1-x)^2} Z_{shunt} \end{aligned} \tag{16}$$

Finally, the total rating of UPQC is determined using equation (12).

B. Rating of I-UPQC

The rating of I-UPQC differs from that of UPQC because when a sag occurs as shown in Fig. 2, the extra power drawn by the PAPF does not pass through the series transformer. On the other hand, the shunt filter voltage, *Vshunt*, is not the same in UPQC and I-UPQC due to the position of SAPF.

The current in series component of the I-UPQC is equal to the load current

$$I_{series} = I_{L1} = I_{L2} = 1.0 \text{ p.u.} \tag{17}$$

and the voltage injected by series component is

$$V_{inj-P} = V_C = x \text{ p.u.} \tag{18}$$

therefore the rating of the SAPF is given by;

$$S_{series} = V_C I_{L1} = x \text{ p.u.} \tag{19}$$

In this case the current of PAPF is the same as (6) and its voltage equals to

$$\begin{aligned} V_{shunt} &= V_s + Z_{shunt} I_{C1} \\ &= (1-x) + \frac{\sqrt{(1-x)^2 + (x-1)\cos^2\phi}}{1-x} Z_{shunt} \end{aligned} \tag{20}$$

and the rating of the shunt part of I-UPQC is calculated by (21),

$$\begin{aligned} S_{shunt} &= V_{shunt} I_{C1} \\ &= \sqrt{(1-x)^2 + (x-1)\cos^2\phi} \\ &+ \frac{(1-x)^2 + (x-1)\cos^2\phi}{(1-x)^2} Z_{shunt} \end{aligned} \tag{21}$$

If the voltage regulation is performed by injecting reactive power into the network, the current of the PAPF is

$$\begin{aligned} I_{C2} &= \sqrt{I_{L2}^2 + I_{S2}^2 - 2I_{L2}I_{S2}\cos(\phi-\theta)} \\ &= \frac{\sqrt{(1-x)^2 + \cos^2\phi - 2(1-x)\cos\phi\cos(\phi-\theta)}}{1-x} \end{aligned} \tag{22}$$

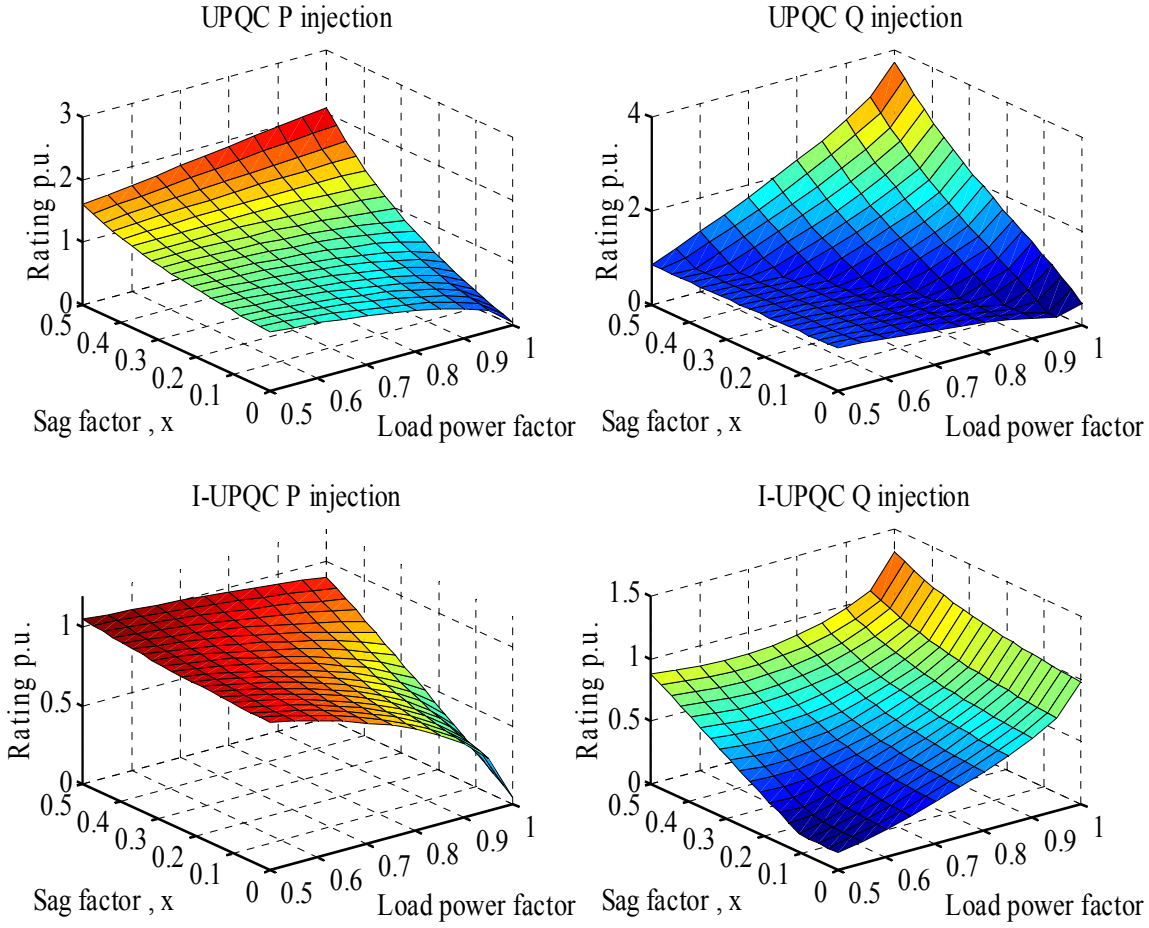

Fig. 8. Rating of UPQC and I-UPQC using active and reactive power injection.

Hence, the voltage and rating of the shunt active power filter is

$$V_{shunt} = (1-x) + \frac{\sqrt{(1-x)^2 + \cos^2\phi - 2(1-x)\cos\phi\cos(\phi-\theta)}}{1-x} Z_{shunt}$$

$$S_{shunt} = (V_S + Z_{shunt} I_{C2}) I_{C2} = \sqrt{(1-x)^2 + \cos^2\phi - 2(1-x)\cos\phi\cos(\phi-\theta)} \cdot \frac{+(1-x)^2 + \cos^2\phi - 2(1-x)\cos\phi\cos(\phi-\theta)}{(1-x)^2} Z_{shunt} \quad (23)$$

The magnitude of voltage injected by SAPF is calculated by (24) using trigonometry

$$V_{inj-Q} = \sqrt{V_{L2}^2 - V_{S2}^2} = \sqrt{x(2-x)}\ p.u. \quad (24)$$

Remembering *IL2* = *Iseries*=1.0 p.u., rating of series filter is

$$S_{series} = V_{inj-Q} I_{series} = \sqrt{x(2-x)}\ p.u. \quad (25)$$

The sum of (23) and (25) yields total rating of I-UPQC when voltage regulation is performed by injecting voltage orthogonal to source current.

A) Comparison

The equations derived in the previous section are used to compare the rating of UPQC and I-UPQC for different power factors. Assume that $0 < \phi < 60°$, (0<PF<1.0), and load rating to be 1.0 p.u.

Fig. 8 shows the results. Rating of the UPQC increases with increasing the level of voltage sag and the load power factor. The rating of I-UPQC in active power injection mode is higher than that of UPQC whereas in reactive power injection mode, has lower rating especially for power factors near unity. Generally, I-UPQC in active power injection mode needs lower rating for compensation of same voltage sag among four cases. With regard to the rating, the following results are provided upon which the proper choice for sag compensation under different values of power factors can be made.

If load power factor is low (near 0.5), using I-UPQC with reactive power injection mode leads to lowest rating.

If load power factor is high(near unity), using I-UPQC or UPQC with active power injection mode leads to lowest rating. However, for deep voltage sags I-UPQC has lower

rating in compare with UPQC.

If load has a moderate power factor (between high and low, around 0.7) and the voltage sag factor is below 0.4, UPQC with reactive power injection yields lowest rating. Fig. 9 concludes the results.

4. Negative Effects of Exchanging Shunt and Series Parts

When UPQC is used, the load current harmonics are compensated before passing through series transformer. On the contrary, in I-UPQC configuration, the harmonics of load current pass through the series transformer and cause deteriorating of this device. On the other hand, when the leakage reactance of the series transformer is high, harmonic components of load current generate a significant amount of voltage harmonics. Suppose that the desirable THD for load voltage is below 5.0%. Therefore, as proved in Appendix A the following inequality must be hold to satisfy this constraint.

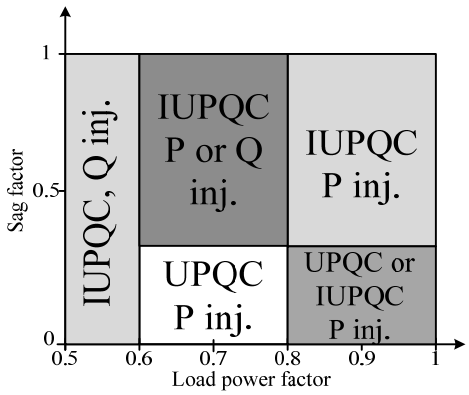

Fig. 9. The lowest rating for different sag factor and load power factor cases (P: active power injection, Q: reactive power injection).

$$X_{leakage} < \frac{0.05}{(\sum_{n=2}^{\infty} n^2 I_{Ln}^2)^{0.5}} \text{ p.u.} \quad (26)$$

where *Xleakage* is the leakage reactance of the SAPF transformer and *ILn* is the *n*th harmonic component of the load current.

Fig. 10 shows the effect of the load current THD on the load voltage THD. As the leakage reactance of the transformer increases, the load current harmonics cause more sever distortion in load voltage. To reduce this effect below the desirable level, *Xleakage* must be maintained below 3.0%.

If the load current contains high frequency harmonics, larger voltage harmonics are produced. As proven in Appendix B the sensitivity of the load voltage THD with respect to load current harmonics is defined by following equation;

$$S_{ILn}^{THD} = \frac{n^2 I_{Ln}}{\sum_{n=2}^{\infty} (nI_{Ln})^2} \text{ for } n \geq \quad (27)$$

The effect of increasing the load current harmonic order on this sensitivity is shown in Fig. 11. When the load current contains high frequency components, its effect on the load voltage THD increases quadratically, therefore, when the load current contains high order harmonics, UPQC configuration is a better choice.

5. Reference Waveform Estimation Strategy

Reference waveforms of shunt and series active power filters of I-UPQC and UPQC can be estimated utilizing various methods. Here a method based on instantaneous reactive power theory is used to generate reference waveforms of the PAPF.

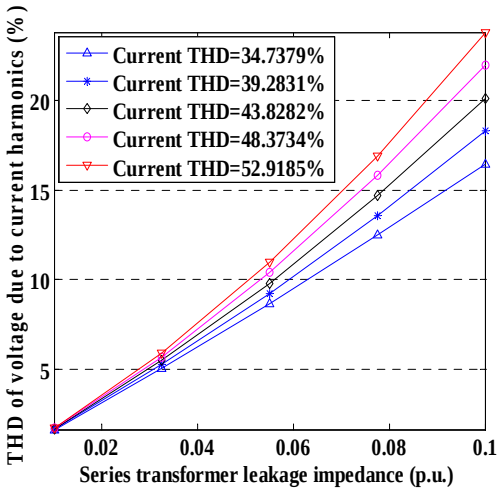

Fig. 10. Effect of load current THD on load voltage THD in I-UPQC configuration.

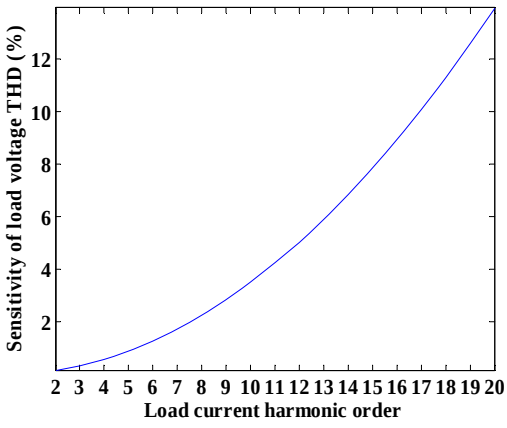

Fig. 11. Sensitivity of load voltage THD to load current harmonic components.

An algorithm based on synchronous reference frame transformation is presented to estimate the reference

waveforms of the SAPF. This method can generate the proper waveforms for both active and reactive power injection cases.

A. SAPF Waveform Estimation

Reference waveform of series part of power quality compensator is the difference between actual voltage of the network and the load ideal voltage according to IEEE-519 standard. An algorithm based on synchronous reference frame transformation is used to generate reference waveforms of SAPF. This method is a modified version of algorithm presented in [11].

Source voltage is transformed into synchronous reference frame by following equation,

$$V_{Sdq0}=\frac{2}{3}\begin{bmatrix}\cos\omega t & \cos(\omega t-120) & \cos(\omega t+120)\\ \sin\omega t & \sin(\omega t-120) & \sin(\omega t+120)\\ 0.5 & 0.5 & 0.5\end{bmatrix}V_{Sabc} \quad (28)$$

To perform in phase and orthogonal voltage compensation, following algorithms are used.

In Phase Voltage Injection: Considering instantaneous phase of network voltage (ωt) as a reference angle, to regulate the load voltage by injecting a nin phase voltage, the ideal source voltage in the synchronous reference frame is

$$v^{*}_{Sdq0}=[V_m \quad 0 \quad 0]^T \quad (29)$$

The load voltage ideal magnitude is shown by *Vm*. The reference voltage of SAPF is

$$v^{*}_{cdq0}=v^{*}_{Sdq0}-v_{Sdq0} \quad (30)$$

To obtain three phase reference voltages, v^{*}_{cdq0} are transformed into the three phase space. Fig. 12 shows the block diagram of the proposed algorithm.

B. Orthogonal Voltage Injection:

Considering orthogonality of d and q axes in the synchronous reference frame, to obtain the voltage compensation by injecting reactive power, the injected voltage should be in phase with q-axis. In the case of using UPQC, due to the PAPF operation, the source current and voltage are in phase. Therefore, if the injected voltage is orthogonal to the source voltage, it is also orthogonal to the source current, so the reactive power injection is provided. Supposing *Vm* to be the ideal magnitude of the load voltage, the reference voltage of the orthogonal method can be calculated as follows:

$$v^{*}_{cd}=v_{Sd} \quad (31)$$

$$v^{*}_{cq}=\sqrt{V_m^2-v_{Sd}^2} \quad (32)$$

Fig. 13 shows the block diagram of the SAPF reference waveform estimation when the injected voltage is orthogonal to the source current.

When the I-UPQC is utilized, the injected voltage is aligned with q-axis which leads to the angle difference of $(\pi/2+\phi-\theta)$ between the load current and the injected voltage which is not equal to $\pi/2$ as shown in Fig. 7. This gives rise to the injection of active power into the network.

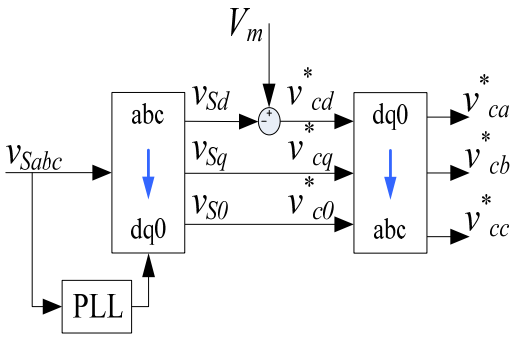

Fig. 12. Block diagram of SAPF reference waveform generation (in phase voltage injection).

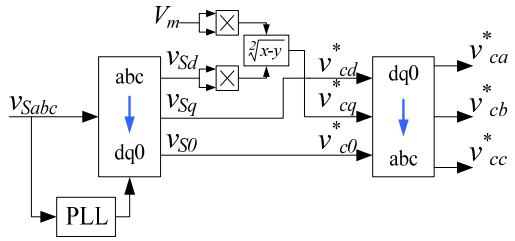

Fig. 13. Block diagram of SAPF reference waveform generation (orthogonal voltage injection).

Assuming |*IL*|=1.0 p.u. and θ as angle between the source and the load voltage after compensation, the injected active power is

$$p_{inj}=\sqrt{x(2-x)}\sin(|\phi-\theta|) \quad (33)$$

Fig. 14 shows this active power as a function of voltage sag magnitude (x) and the load power factor.

By using the orthogonal voltage algorithm, the injection of active power is less in compare with the in phase method when the sag factor *x* is above 0.3 p.u. and the power factor is below 0.9. However, the maximum of injected active power is less when in phase method is used. To reduce the active power which is injected by SAPF, the angle between fundamental component of the load current and the source voltage (power factor) must be known.

Orthogonal voltage injection leads to load voltage phase jump. The amount of this phase jump (ξ) rises as the amplitude of the sag increases, i.e.,

$$\xi=\tan^{-1}\frac{v^{*}_{cq}}{v_{Sd}} \quad (34)$$

Fig. 15 shows the variations of load voltage angle due to the occurrence of the voltage sag. If the load is sensitive to phase jumps, it will encounter problems especially when the voltage sag has a large amplitude.

C. Waveform Estimation

Assuming the vectors of the network voltage and the load current as

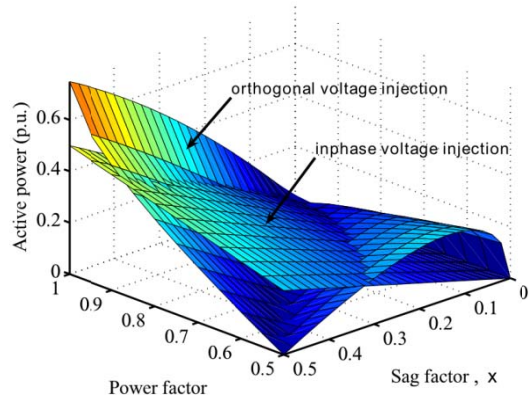

Fig. 14. Comparison between active power injected into the network using in phase and orthogonal voltage injection method.

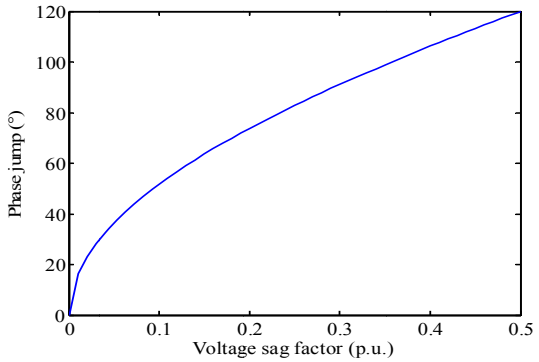

Fig. 15. Phase jump due to injection of orthogonal voltage.

$$\vec{v}_S = [v_{Sa} \quad v_{Sb} \quad v_{Sc}]^T \tag{35}$$

$$\vec{i}_l = [i_{la} \quad i_{lb} \quad i_{lc}]^T \tag{36}$$

the active and reactive power of load are equal to the dot and cross product of voltages and currents respectively, i.e.,

$$p = \vec{v}_S \vec{i}_l = v_{Sa} i_{la} + v_{Sb} i_{lb} + v_{Sc} i_{lc} \tag{37}$$

$$q = \vec{v}_S \times \vec{i}_l = [q_a \quad q_b \quad q_c]^T \tag{38}$$

the mean reactive power is defined as

$$q_{ave} = \frac{q_a + q_b + q_c}{\sqrt{3}} = \frac{v_{Sa}(i_{lb} - i_{lc}) + v_{Sb}(i_{lc} - i_{la}) + v_{Sc}(i_{la} - i_{lb})}{\sqrt{3}} \tag{39}$$

Active and reactive power consist of a constant and an oscillatory component as,

$$p = \bar{p} + \tilde{p} \tag{40}$$

$$q = \bar{q} + \tilde{q} \tag{41}$$

where $\bar{p}$ and $\bar{q}$ are constant and $\tilde{p}$ and $\tilde{q}$ are oscillatory components.

1) In phase voltage injection

Assuming that the PAPF compensates all reactive power demand of the load, by generating q, and also to compensate the active power oscillations of the load current by generating $\tilde{p}$. Hence, $\tilde{p}$ is estimated by passing p through a low pass filter.

The voltage at DC link capacitor to be kept constant for achieving the proper compensation [12]. Hence, PAPF should draw additional active power from network to regulate the DC link capacitor voltage. Swings in capacitor voltage are due to distortions exist in network voltage, internal switching and the copper losses of transformer. The voltage error which is Difference between the actual capacitor voltage and its reference is fed into a PI controller. This controller estimates the required amount of active power (*ploss*) for regulating the capacitor voltage. The total active power drawn by PAPF is defined by

$$p_T = \tilde{p} + p_{loss} \tag{42}$$

Reference currents of three phases of the shunt active power filter are attained by (43) and its block diagram is shown inFig..

$$i_{ca}^* = i_{la} - \frac{p_T}{v_a^2 + v_b^2 + v_c^2}$$

$$i_{cb}^* = i_{lb} - \frac{p_T}{v_a^2 + v_b^2 + v_c^2} \tag{43}$$

$$i_{cc}^* = i_{lc} - \frac{p_T}{v_a^2 + v_b^2 + v_c^2}$$

If the PAPF of the power quality conditioner injects these currents into the network, the harmonics and the reactive component of the load will diminish, and the DC link voltage is kept constant.

2) Orthogonal voltage injection

The algorithm described in the previous section compensates the reactive power considering that the load and the source voltages are in phase. As shown in Fig. 7, by using the orthogonal voltage injection, the load voltage leads the source during voltage sag. Fig. 15 shows the value of the phase angle difference between the source and load voltage. This will lead to injection or absorption of extra reactive power into/from the network by PAPF depending on the sign of $(\phi - \theta)$. If $(\phi - \theta)$ is positive, the source current will lead the source voltage so PAPF injects extra reactive power into the network. Over rating of PAPF and unwanted distribution network reaction such as over voltage is the result. To solve this problem, a PI controller

is used for estimation of additional reactive power. The error voltage i.e., the difference between amplitude of the source voltage in d-axis and its nominal value is fed into this controller and the output is considered as an extra reactive power.

Assuming $\bar{q}$ as the output of PI controller, reference waveforms of PAPF are as follows;

$$
\begin{aligned}
i_{ca}^{*} &= i_{la} - \frac{1}{v_a^2+v_b^2+v_c^2}\left(v_{Sa}.p_T + \frac{\bar{q}}{3}(v_{Sc}-v_{Sb})\right)\\
i_{cb}^{*} &= i_{lb} - \frac{1}{v_a^2+v_b^2+v_c^2}\left(v_{Sb}.p_T + \frac{\bar{q}}{3}(v_{Sa}-v_{Sc})\right) \qquad (44)\\
i_{cc}^{*} &= i_{lc} - \frac{1}{v_a^2+v_b^2+v_c^2}\left(v_{Sc}.p_T + \frac{\bar{q}}{3}(v_{Sb}-v_{Sa})\right)
\end{aligned}
$$

Fig. 17 shows the block diagram of the reference waveform generation algorithm for PAPF. By using this method, the phase difference between the load and source voltage no longer causes the unwanted reactive power flow through the network and the compensator.

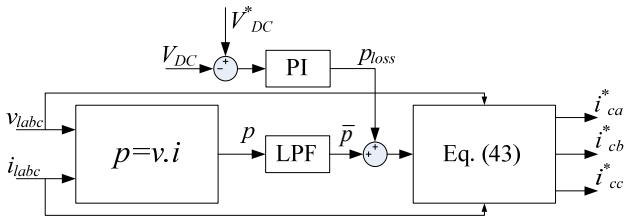

Fig. 16. Shunt active power reference waveform estimation for in phase voltage injection.

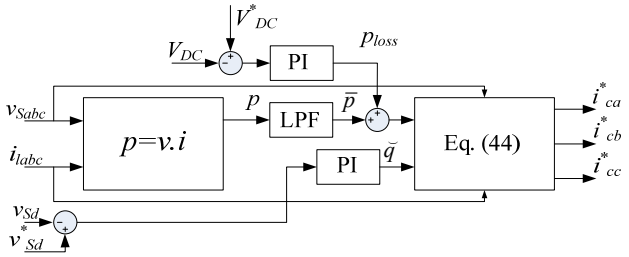

Fig. 17. Shunt active power reference waveform estimation for orthogonal voltage injection.

6. Simulation Results

Using PSCAD/EMTDC software package, two configurations of power quality conditioners under the control of the aforementioned algorithms are simulated. A full-bridge three phase rectifier is used as a nonlinear load and simulations are performed at 20kV level. The compensator and the load parameters are shown in Table I.

Case A: Current Compensation

Fig. 18 shows the load current and the source current after compensation made by UPQC and I-UPQC. The load current consists large of amount of harmonics with order $6n\pm1; n=1,2,3,\ldots$. The magnitude of the load current harmonics is 20% for 5th and 8.0% for 7th harmonic. The uncompensated source current is equal to the load current. The compensated source current is nearly sinusoidal having THD about 1.3% and 1.7%, respectively in UPQC and I-UPQC.

Case B: Voltage Sag Compensation by Injecting Active Power

Operation of two compensators during voltage sag and swell is shown in Fig. 19. The magnitude of the source voltage is reduced by 25% at 0.09 s and is increased by same amount at 0.15 s. Using in phase voltage injection, both configurations regulate the load voltage. However, by considering the same rating for shunt and series part in both devices, I-UPQC shows better performance during sag and swell. The UPQC creates voltage disturbances at instant 0.06 sec when it begins to start voltage compensation, and also the same happens at 0.09 and 0.15 s during voltage sag and swell. Series part of UPQC needs greater rating to operate smoothly and without disturbances in the case of sag and swell occurrence.

Table 1. Load and compensator parameters.

Load	
Load rating	5 MW, 1.3 MVAR
Load Voltage	63 kV
Load transformer	Y/Δ, 20-6.3 kV, 5 MVA
Compensator	
DC link capacitor	700 μF, 40 kV
Series transformer	3×one-phase, 3 MVA, 10-20 kV
Series VSI switching drive	PWM, fswitching = 10 kHz
Shunt transformer	Y/Y, 20-20 kV
Shunt VSI switching drive	Hysteresis, Hysteresis band = 0.01

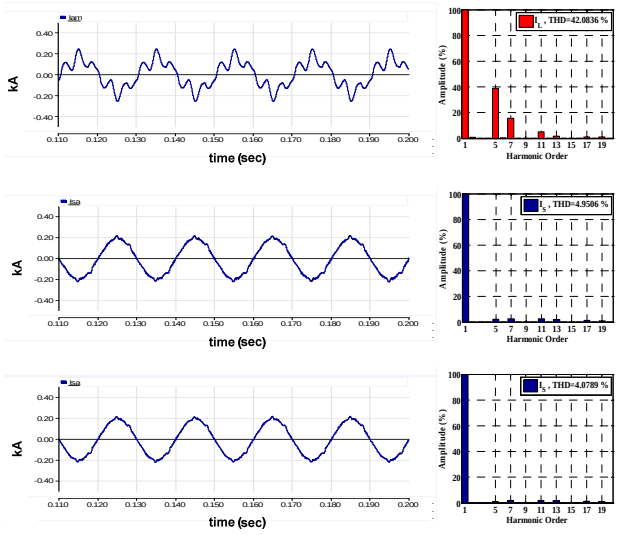

Fig. 18. From top to bottom: load current, source current compensated by UPQC, source current compensated by I-UPQC.

Case C: Voltage Sag Compensation by Injecting Reactive Power

To access the compensator performance in voltage compensation by injecting orthogonal voltage, a voltage sag as deep as 25%, started at t = 0.1 sec is supposed. Fig. 20 shows the load voltages after compensation made by UPQC and I-UPQC. The load voltage is regulated, however a

phase jump about 41° is observed at the beginning of the voltage sag.

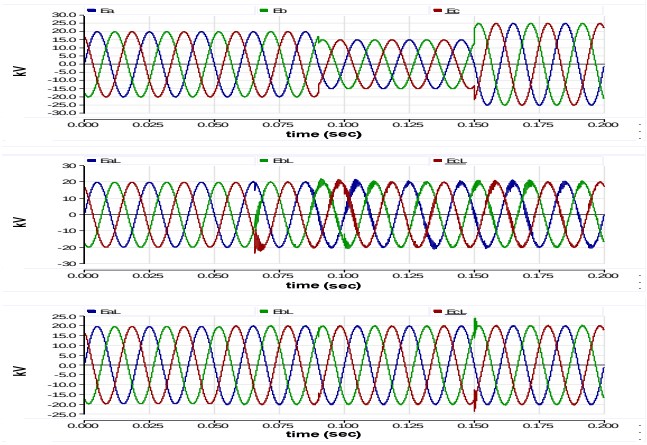

Fig. 19. Voltage compensation using in phase voltage injection; from top to bottom: source voltage, load voltage compensated by UPQC, load voltage compensated by I-UPQC.

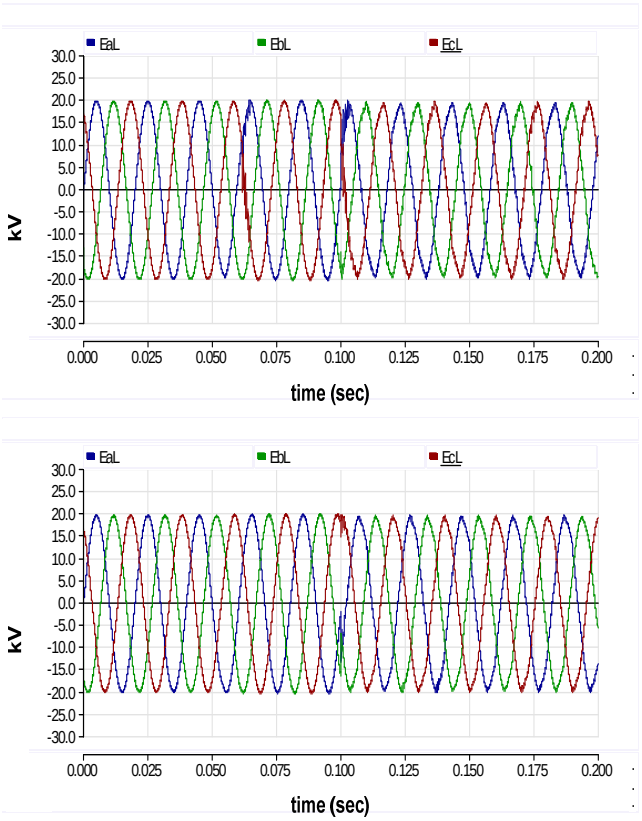

Fig. 20. Voltage compensation using orthogonal voltage injection; load voltage compensated by UPQC (top), load voltage compensated by I-UPQC (bottom).

Case D: Effect of Orthogonal Voltage Injection on Load Current

Fig. 21 shows the effect of voltage compensation on load current when voltage regulation is performed by reactive power injection. The source voltage is dropped at instant 0.09 sec. The UPQC with in phase current injection causes phase difference between the source voltage and current. In contrary, the orthogonal current injection method eliminates phase difference between the source current and voltage, so the source does not supply any reactive power.

As discussed in Section. V-A, the voltage regulation using I-UPQC with proposed algorithm is not achieved by pure reactive power injection. Fig. 22 shows the angle between the voltage of the series transformer and its current during the compensation of voltage sag. The phase difference between the voltage and current of SAPF part of the UPQC is about 90° but it is near 68° for the I-UPQC as predicted by (34).

The load power factor is 0.95 lag, which leads to $|\phi-\theta|=23°$ displacement angle between the injected voltage and the load current.

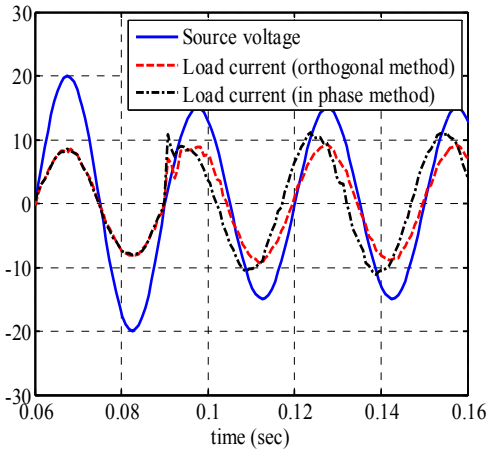

Fig. 21. Source voltage and current compensated by UPQC using in phase and orthogonal current control algorithms.

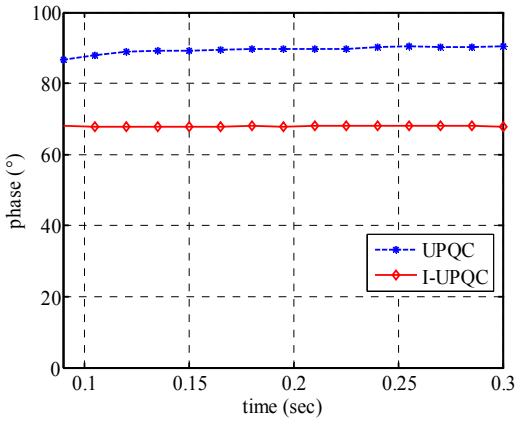

Fig. 22. Phase difference between injected voltage and series transformer current.

Case E: Effects of Source Voltage Unbalance on Current Compensation

Considering the configuration of the UPQC, the voltage of PAPF is pre-regulated by SAPF, so the current compensation is not affected by voltage distortions. On the other hand, the PAPF of the I-UPQC is directly connected to the network so the voltage distortions affect its operation. The algorithm described in Section V-B for controlling PAPF is not robust against voltage distortions. Fig. 23 shows the source voltage and current when the network voltage is unbalance. The voltage of phase b is 25% lower

than other phases and contains 6.5% positive and zero sequence components. By using UPQC, the magnitudes of the source current harmonics are nearly reduced to an acceptable limit (THD about 6%). Where as I-UPQC is not able to reduce source current harmonics effectively. The source current contains 15% third harmonic and the total harmonic distortion is 12%. So the I-UPQC configuration can not compensate current distortions in the presence of the network voltage distortions. To overcome this problem the control algorithm of the PAPF to be such that not affected by the source voltage distortions [13].

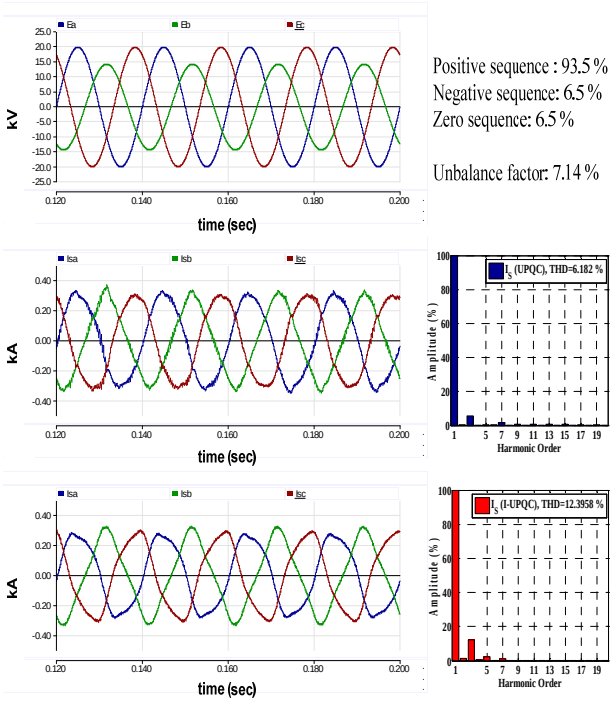

Fig. 23. From top to bottom: source voltage (unbalanced), source current compensated by UPQC, source current compensated by I-UPQC.

7. Conclusion

Using the mathematical representations it is shown that if the series part of UPQC is interchanged with its shunt part such that the series part is located at load side (known as I-UPQC), the total rating of the compensator will be reduced when the load draws a large amount of reactive power from the network. Further rating reduction is possible by using reactive power injection for voltage regulation.

The negative effects of modifying UPQC into I-UPQC on the load voltage harmonics is analyzed using sensitivity of the load voltage THD to the load current harmonics. It is shown that the SAPF transformer leakage reactance must be kept as low as possible to reduce the load voltage THD.

A new algorithm has been presented for generating reference waveforms of the UPQC and the I-UPQC for orthogonal voltage injection to avoid phase jump. Numerical simulations show that the I-UPQC can perform power quality compensation using conventional control algorithm if the network voltage does not contain significant unbalance or harmonics.

Appendix A

The load voltage THD is,

$$THD_{v_L} = \frac{\sqrt{\sum_{n\geq 2} V_{Ln}^2}}{V_{L1}} \qquad (A-1)$$

where n is the harmonic order. The harmonic components of the load voltage caused by the load current voltage drop across the series transformer leakage reactance is

$$V_{Ln} = nX_{leakage} I_{Ln}. \qquad (A-2)$$

Supposing $VL1$ = 1.0 p.u. and substituting (A-2) in (A-1) we have

$$THD_{V_L} = \sqrt{\sum_{n\geq 2} (nX_{leakage} I_{Ln})^2}. \qquad (A-3)$$

If the maximum load voltage permitted THD is 5% (THDVL<5.0) and after some manipulations

$$X_{leakage} < \frac{0.05}{\sqrt{\sum_{n\geq 2} (nI_{Ln})^2}} \text{ p.u.} \qquad (A-4)$$

Appendix B

The load voltage THD sensitivity function in respect to the load current is,

$$S_{ILn}^{THD} = \frac{I_{Ln}}{THD} \frac{\partial THD}{\partial I_{Ln}} \qquad (B-1)$$

Substituting (A-4) in (B-1) we have

$$S_{ILn}^{THD} = \frac{n^2 I_{Ln}}{\sum_{n=2}^{\infty} (nI_{Ln})^2} \text{ for } n \geq 2 \qquad (B-2)$$

References

[1] G. J. Nilesen and F. Blaabjerg, "A detailed comparison of system topologies for dynamic voltage restorer," *IEEE Transactions on Industry Application*, vol. 41, no. 5, pp. 1272–1280, September/October 2005.

[2] B. Singh, K. Al-Haddad and A. Chandra, "A review of active filters for power quality improvement," *IEEE Transactions on Industrial Electronics*, vol. 46, no. 5, p. 960, 971 1999.

[3] P. Mattavelli, "A closed-loop selective harmonic compensation for active filters," *IEEE Transactions on Industry Application*, vol. 37, no. 1, pp. 81–89, January/February 2001.

[4] M. J. Newman, D. G. Holmes, J. G. Nilesen, and F. Blaajberg, "A dynamic voltage restorer DVR with selective harmonic compensation at medium voltage

level," *IEEE Transactions on Industry Application*, vol. 41, no. 6, pp. 1744–1453, November/December 2005.

[5] D. M. Vilathgamuwa, A. A. D. R. Perera, and S. S. Choi, "Voltage sag compensation with energy optimized dynamic voltage restorer," *IEEE Transactions on Power Delivery*, vol. 18, no. 3, pp. 928–936, Jul. 2003.

[6] Y. Y. Kolhatkar and S. P. Das, "Experimental investigation of a single-phase UPQC with minimum VA loading," *Electric Power System Research*, vol. 77, pp. 821–830, Mar./Apr. 2007.

[7] H. Fujita and H. Akagi, "The unified power quality conditioner: the integration of series and shunt active power filters," *IEEE Transactions on Power Electronics*, vol. 13, no. 2, pp. 315–322, Mar. 1998.

[8] L. M. Tolbert and P. Z. Peng, "A multilevel converter based universal power conditioner," *IEEE Transactions on Industrial Applications*, vol. 36, no. 2, pp. 596–603, Mar./Apr. 2000.

[9] S. Srinath, M. P. Selvan, and K. Vinothkumar, "Comparative evaluation of performance of different control strategies on UPQC connected distribution system," *5th International Conference on Industrial and Information Systems*, India, pp. 502–507, Jul. 2010.

[10] M. Basu, S. P. Das and G. K. Dubey, "Comparative evaluation of two models of UPQC for suitable interface to enhance power quality," *Electric Power System Research*, vol. 77, pp. 821–830, Mar./Apr. 2007.

[11] M. Hu and H. Chen, "Modeling and controlling of unified power quality compensator," *IEEE Conference on Advances in Power System Control*, *Operation and Management*, vol. 2, pp. 431–435, 2000.

[12] J. Tutunen, M. Salo and H. Tuusa, "The influence of the DC-link voltage control on the current harmonic filtering of the series hybrid active filters," *31th Annual Conference on Industrial Electronics Society*, 2005, pp. 918–923.

[13] S. B. Karanki, M. K. Mishra, and B. K. Kumar, "Particle swarm optimization-based feedback controller for unified power-quality conditioner," *IEEE Transactions on Power Delivery*, vol. 25, no. 4, pp. 2814–2824, Oct. 2010.

Mohamad Hosseini Abardeh received the B.Sc. degree in control engineering from Ferdowsi university of Mashhad in 2005, and the M.Sc. degree in power engineering from Tarbiat Modares University of Tehran, Iran in 2008. He is currently a Ph.D. student at the Ferdowsi University of Mashhad. His research interests are power electronic, power quality and renewable energies.

Reza Ghazi was born in Semnan, Iran in 1952. He received his B.Sc., degree (with honors) from Tehran University of Science and Technology, Tehran, Iran in 1976. In 1986 he received his M.Sc. degree from Manchester University, Institute of Science and Technology (UMIST) and the Ph.D. degree in 1989 from University of Salford UK, all in electrical engineering. Following receipt of the Ph.D. degree, he joined the faculty of engineering Ferdowsi University of Mashhad, Iran as an Assistant Professor of electrical engineering. He is currently Professor of Electrical Engineering in Ferdowsi University of Mashhad, Iran. His main research interests are reactive power control, FACTS devices, application of power electronic in power systems, distributed generation, restructured power systems control and analysis. He has published over 100 papers in these fields including three books.